

# Tribological Properties of Ni-P Electroless Coatings on Low-Carbon Steel Substrates Using an Environmentally Friendly Pretreatment

W. H. Lee<sup>1,2</sup>, C.H. Huang<sup>3</sup>, Y. T. Sun<sup>1,2</sup>, H. Chang<sup>1,2,\*</sup>, C. Y. Hsu<sup>3\*</sup>

<sup>1</sup> Graduate Institute of Manufacturing Technology, National Taipei University of Technology, Taipei, Taiwan

<sup>2</sup> Department of Mechanical Engineering, National Taipei University of Technology, Taipei 10608, Taiwan

<sup>3</sup> Department of Mechanical Engineering, Lunghwa University of Science and Technology, Taoyuan 33306, Taiwan

\*E-mail: [f10381@ntut.edu.tw](mailto:f10381@ntut.edu.tw), [cyhsu@mail.lhu.edu.tw](mailto:cyhsu@mail.lhu.edu.tw)

Received: 18 August 2017 / Accepted: 25 October 2017 / Published: 28 December 2017

---

This study deposits Ni-P alloy films coatings onto low carbon steel substrates using an electroless process. The coating's morphology and properties, including the hardness, polarization and frictional behavior, are analyzed. A conventional pretreatment that uses roughening and activation steps ensures better adhesion between the Ni-P plated layer and the substrate and renders the substrates catalytic. This study reports an environmentally friendly pretreatment for the substrates: physical sandblasting (using emery powder particles) and oxygen plasma etching. XRD analysis shows that the diffraction pattern for the Ni-P alloy exhibits a wider peak, which indicates that there is an amorphous phase. SEM micrographs after electroless Ni-P plating that uses plasma etching show that the surface is more even and fairly smooth, which indicates good Ni-P film characteristics. The experimental results show that a plasma etching pretreatment for coating with Ni-P film increases the hardness and corrosion resistance and reduces the coefficient of friction.

---

**Keywords:** electroless plating, substrates pretreatment, Ni-P films, sandblasting, plasma etching.

## 1. INTRODUCTION

Of the various surface treatment techniques for surface modification, electroless nickel phosphorus (Ni-P) alloy coating on metals and alloys by chemically autocatalytic reduction is an easy and cheap process [1,2]. These hard coatings are used in various industrial fields, such as chemical engineering, mechanical engineering, the automobile, electronics, aerospace and the oil and gas

industries [3]. They have excellent properties, including uniform coating thickness, good anticorrosive performance and superior wear resistance and they exhibit good electrical and thermal conductivity [4]. There are many applications for electroless Ni–P coating in engineering because it can be used for complicated component surfaces and many substrates, such as steel, aluminum alloy, magnesium alloy, silicon, brass and glass. [5]. The properties of Ni–P coatings can also be improved by doping with various types of particulates, to fabricate multifunctional composite materials [6]. Carbon steels are widely used in various industrial fields because of their high strength, ease of machining, and welding and low price [7]. However, their industrial applications in numerous fields where high corrosion resistance is required are limited, because low-carbon steel is easily corroded in real conditions. In order to prevent carbon steel from corroding, many protective coatings are used [8]. Yang et al. [9] reported that plasma electrolytic oxidation increases the adhesion strength by forming a sub-layer for the organic coating on low-carbon steel, increases corrosion resistance and allows a longer service life in a corrosive environment. Liew et al. [10] analyzed the tribological and scratch performance of low-carbon steel (LCS) substrates with and without Ni–P–PTFE (PTFE, poly tetra fluoro-ethylene) coatings. It is significant that the duration of heat treatment for Ni–P–PTFE coating affects friction and wear. The PTFE (or  $WS_2$ ,  $MoS_2$ ) particles are co-deposited into a Ni–P matrix because electroless Ni–P plating uses the particles' solid lubricants to reduce the coefficient of friction, which increases resistance to corrosion and increases wear resistance [11]. Xiang et al. [12] determined the effect of current density on wettability and corrosion resistance for a nickel coating on a LCS surface. For a current density of  $6\text{ A/dm}^2$ , a super-hydrophobic coating significantly improves the corrosion resistance of LCS. Yang et al. [13] reported that electroless Ni–P coating significantly reduces the coefficient of thermal expansion (CTE) for carbon steel. The diffusion layer (mainly  $FeNi_3$ ) plays a key role in inhibiting the thermal expansion of the iron substrate (named the diffusion-layer inhibitory mechanism). This decrease in the CTE applies to all ferrous alloys.

This study determines the abrasive and erosive wear behavior of LCS substrates that are coated with Ni–P alloy films using an electroless process. To ensure that the substrates are catalytic, a conventional pretreatment uses roughening and activation steps, prior to electroless plating. This ensures better adhesion between the Ni–P plating layer and the substrate. To reduce chemical pollution in the environment, an environmentally friendly pretreatment is used for the substrates. The pretreatment parameters for the different LCS substrates before the electroless coating of the Ni–P alloy: The LCS substrates are subjected to different pretreatments. Sample 1 has conventional pretreatment roughening (15%  $H_2SO_4$ , 10 min) and then activation (10%  $H_2SO_4$ , 30 sec). Sample 2 has physical sandblasting (using emery powder particles), sandblast air pressure =  $5\text{ kg/cm}^2$ , emery powder = 24 mesh, duration time = 10 min. Sample 3 has physical oxygen plasma etching, base pressure =  $1.0 \times 10^{-5}$  torr, working pressure =  $4.5 \times 10^{-3}$  torr, direct current power = 100 Watt, duration time = 10 min.

The electroless Ni–P plating parameters: Samples 1, 2 and 3 use the same electroless plating parameters. The plating bath contains nickel sulfate ( $NiSO_4 \cdot 6H_2O$ ), sodium hypophosphite ( $NaH_2PO_2 \cdot H_2O$ ) and sodium succinate ( $Na_2C_4H_4O_4 \cdot 6H_2O$ ). The plating temperature is  $90^\circ C$ , the pH value is 5 and the plating time is 10 min. The mechanical properties and corrosion resistance are

measured, in order to determine the effect of the electro-less Ni–P coatings on the tribological performance of the LCS substrate.

## 2. EXPERIMENTAL PROCEDURE

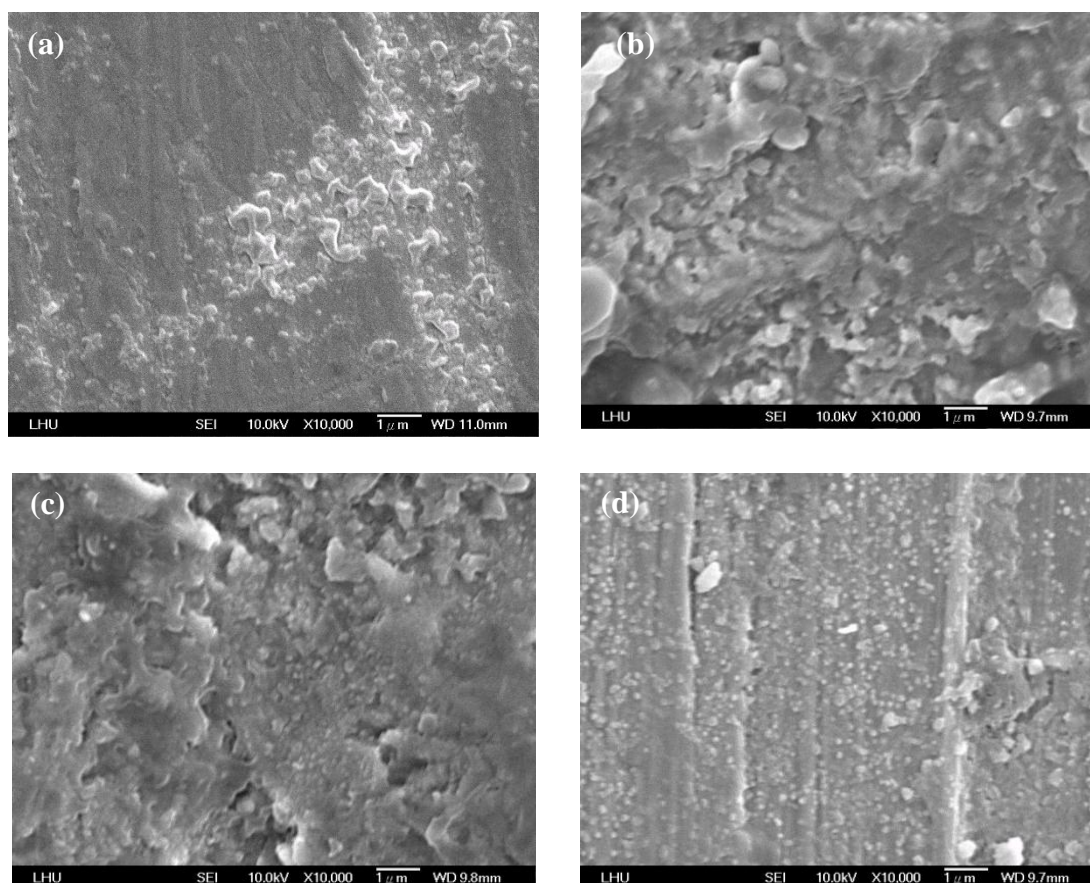
The substrate material was LCS (30 mm×30 mm×1 mm), with a chemical composition (wt.%) of 0.05 C, 0.15 Si, 0.15 Mn, 0.01 S, 0.02 P, 0.04 Al and 0.01 Ni, with the remainder being Fe. The samples were progressively mechanically polished using 100 to 1200 grit papers. The substrates were then rinsed in acetone, ethanol and deionized water for 7 min and ultrasonically cleaned, in order to degrease and clean the surfaces. For comparison purposes, three different types of substrate pretreatment were applied before electro-less deposition: roughening and then activation (sample 1), sandblasting (sample 2) and oxygen plasma etching (sample 3). This was followed by electroless plating, using the same parameters. The frictional properties of the coated and uncoated specimens were determined using wear tests that used a ball-on-disc tribometer (CSM Instruments, Switzerland) [14]. The tests were conducted using no lubricant along a circular track of 2.2 mm in diameter against a 6.0 mm diameter Al<sub>2</sub>O<sub>3</sub> ball at 0.075 m/s, using a normal load of 2.0 N and in an ambient atmosphere. The corrosion behavior of the electroless Ni–P films was determined using anodic potentiodynamic polarization tests. A potentiostat/galvanostat apparatus (EG&G model 263A, USA) and a 3.5 wt.% NaCl solution of corrosive medium were used to simulate an aggressive aqueous environment containing Cl<sup>-</sup> ions. A standard saturated calomel electrode was used as a reference electrode and platinum (20 mm×20 mm) was used as a counter (or auxiliary) electrode. In all cases tested, the working areas were 100 mm<sup>2</sup> and carried out at ambient temperature. The electrode potential was increased from -1.0 V to 0.4 V at a scanning rate of 1 m V/s.

The corrosion potential ( $E_{corr}$ ) and corrosion current density ( $I_{corr}$ ) were respectively measured using the polarization curve and the Tafel extrapolation method [15]. The film thickness was measured using a surface profilometer ( $\alpha$ -step, ET-4000A). The morphology was determined using a field emission scanning electron microscope (SEM, JEOL JSM-6500F). The chemical composition of the films was measured using an Energy dispersive spectrometer (EDS). The films' structural properties were determined using X-ray diffraction (Rigaku-2000 X-ray Generator), with Cu Ka radiation (40 kV and 30 mA,  $\lambda = 0.1541$  nm) and a grazing incidence angle of 1°.

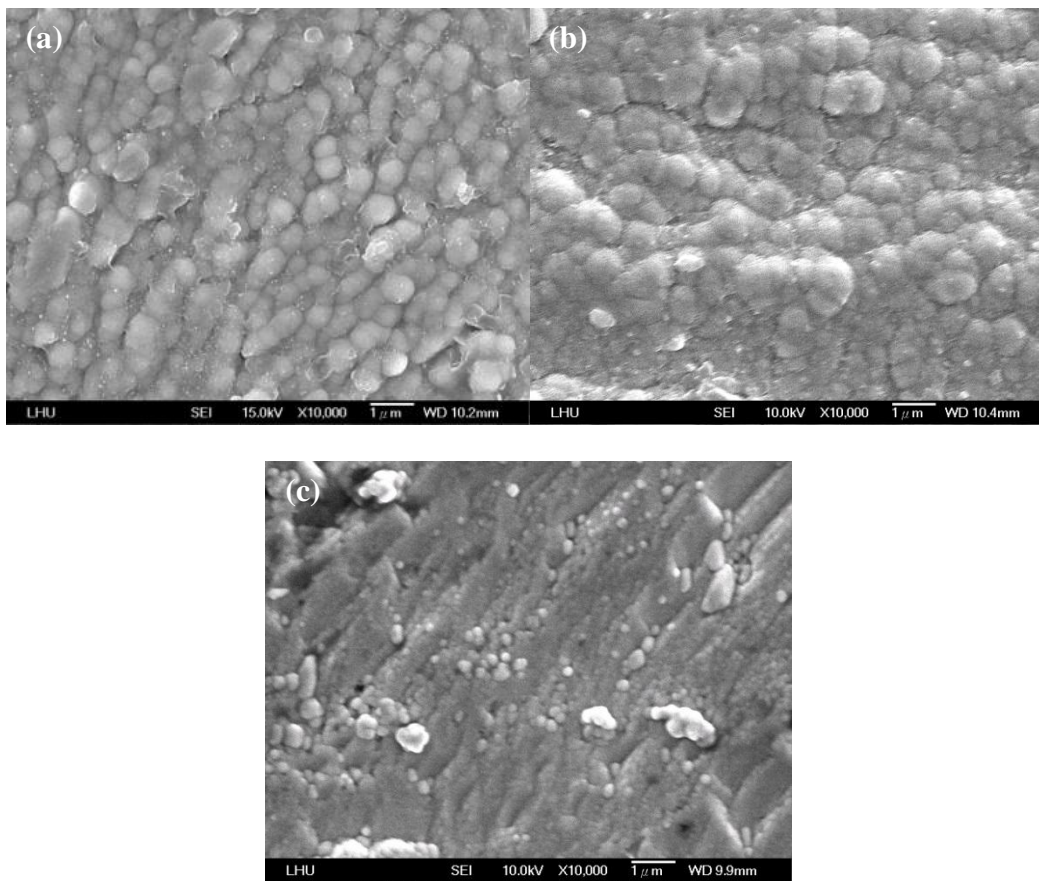
## 3. RESULTS AND DISCUSSION

Fig. 1 shows the SEM surface morphology of the LCS substrates, without and with pretreatments, before the electro-less plating. In Fig. 1 (a), the original LCS substrate exhibits some slight polishing scratches and there are particles on the surface. However, this is not suitable for subsequent electro-less plating. Fig. 1 (b) shows that the surface of the sample becomes rough after activation using sulfuric acid, which improves the adhesion of the Ni–P coatings and renders the surface more chemically active. When the LCS substrates surfaces are sandblasted for 10 min (using emery powder particles), a rough surface structure formed, as shown in Fig. 1 (c). After plasma etching, there is slight pitting and micro-roughness on the surface (Fig. 1 d). These substrate pretreatments increase the hydrophilic character and surface roughness of the substrates, which

anchors Ni–P film during the electroless plating process [16]. The typical surface micromorphology for the electroless Ni–P coated samples is determined as a function of the substrate pretreatments using SEM, as shown in Fig. 2. The substrate surface is fully covered by the coatings. Different pretreatment methods produce different structures. The electroless Ni–P layers are compact, uniform and exhibit a typical spherical nodular structure. There are no obvious flaws or apertures on the coating surface, but the pretreatments affect their size and distribution (Fig. 2 a and b). Fig. 2 (c) shows the Ni–P film that result from plasma etching. The surface is more even and fairly smooth, which indicates good Ni–P film characteristics. In Fig. 3, the XRD analysis shows that the diffraction pattern for the Ni–P binary alloy has a broad peak, which indicates that the structure of the coating is amorphous. Fig. 3 shows the XRD crystal structures for the Ni–P binary alloy coating. It is seen that there is only one peak at  $2\theta=45.02^\circ$ , which is ascribed to the (111) plane diffraction of crystalline Ni. The wide peak indicates that the structure of the coating has an amorphous phase in the samples. These results are consistent with those of Li et al. [17], and may be due to the lattice disorder that is caused by phosphorous atoms in the coating structure. The chemical composition of the coatings, as determined from EDS analysis, shows that only Ni (88.83 wt%) and P (11.17 wt%) are detected. No other elemental signal is seen in Fig. 4.



**Figure 1.** SEM micrographs of LCS substrates that use the three pretreatments before electroless plating: (a) original substrates, (b) roughening activation using sulfuric acid (sample 1), (c) sandblasting (sample 2) and (d) oxygen plasma etching (sample 3).



**Figure 2.** SEM micrographs taken after electroless Ni–P plating for each substrate pretreatment corresponding to Fig. 1: (a) roughening activation using sulfuric acid (sample 1), (b) sandblasting (sample 2) and (c) plasma etching (sample 3).

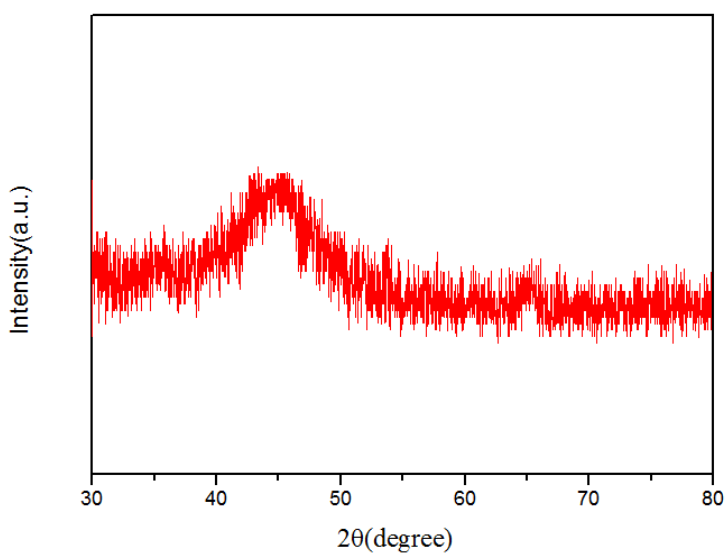


**Figure 3.** X-ray diffraction patterns for the electroless Ni–P coatings.

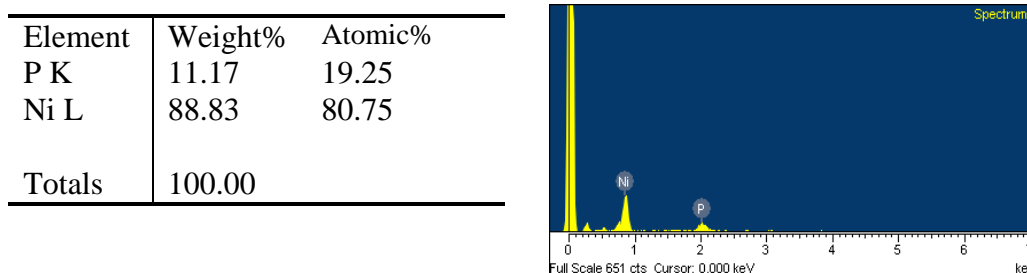


**Figure 4.** EDS analysis of the electroless Ni–P coating.

This study uses electroless Ni–P film with a thickness of about 9.41 μm. The mechanical properties of the samples were determined using a hardness test, a corrosion test and a tribological test. The micro-hardness of the uncoated and coated LCS substrates was determined. The original LCS substrate has a low microhardness value of 133 HV. This hardness increases significantly after coating with a Ni–P film. The respective microhardness values for the film samples 1, 2 and 3 are 254, 293 and 299 HV. These are approximately twice as good as the uncoated counterparts.

Polarization tests were performed using a 3.5 wt.% NaCl solution at room temperature. The polarization curves for uncoated and coated (samples 1, 2 and 3) were derived from the relationship between the corrosion potential ( $E_{corr}$ ) and the corrosion current density ( $I_{corr}$ ), which is commonly used as an index to evaluate the kinetics of corrosion resistance using the Tafel equation [18], as shown in Fig. 5.

$$\text{Tafel equation [18]} \quad \beta = (\beta_a \times \beta_c) / [2.3(\beta_a + \beta_c)] \dots\dots\dots(1)$$

$$R_p = (\beta_a \times \beta_c) / [2.3(\beta_a + \beta_c) I_{corr}] \dots\dots\dots(2)$$

where  $\beta_a$  and  $\beta_c$  are the anodic and cathodic Tafel slope, respectively.

$\beta$  and  $R_p$  are the Tafel constant and polarization resistance, respectively.

It is seen that for all cases, there are both anodic and cathodic branches of the polarization curve. The polarization curves were used to estimate the  $I_{corr}$ , by Tafel extrapolation of the cathodic branch to the  $E_{corr}$ . The polarization test ( $\beta_a$ ,  $\beta_c$ ,  $\beta$ ,  $R_p$ ,  $I_{corr}$  and  $E_{corr}$ ) results are summarized in Table 1. It is evident the electroless Ni–P plating that replaces the roughening then activation (sample 1) pretreatments with sandblasting (sample 2) and plasma etching (sample 3) leads to increased corrosion resistance. Compared with the uncoated LCS specimen ( $E_{corr} = -0.50$  V), the electroless Ni–P coated samples exhibit higher  $E_{corr}$  values in the range  $-0.44$  to  $-0.37$  V. A higher  $E_{corr}$  value denotes that a stable electrode potential has been achieved and is evidence that the coated LCS substrates have greater corrosion resistance. The higher the polarization resistance ( $R_p$ ), the more corrosion resistant is the material. The  $R_p = 21.56 \mu\text{Ohms}/\text{cm}^2$  for uncoated LCS increased significantly from 29.77 to 69.87  $\mu\text{A}/\text{cm}^2$  after coating with a Ni–P film. The smaller the corrosion current ( $I_{corr}$ ), the more corrosion resistant is the material. The corrosion current density  $I_{corr} = 1.97 \mu\text{A}/\text{cm}^2$  for uncoated LCS decreases significantly from 1.53 to 0.38  $\mu\text{A}/\text{cm}^2$  after coating with a Ni–P film. It is noteworthy that the anodic and cathodic current density for LCS substrates is significantly reduced when they are coated with a Ni–P film. Plasma etching pretreatment and coating with a Ni–P film (sample 3) gives the good corrosion resistance in the polarization test. Fig. 6 shows the SEM micrographs for electroless plated

samples after the corrosion test for various substrate pretreatments. It is seen that the Ni-P film coating uses conventional roughening then activation has more micro pores or micro cracks than those that use sandblasting or plasma etching.

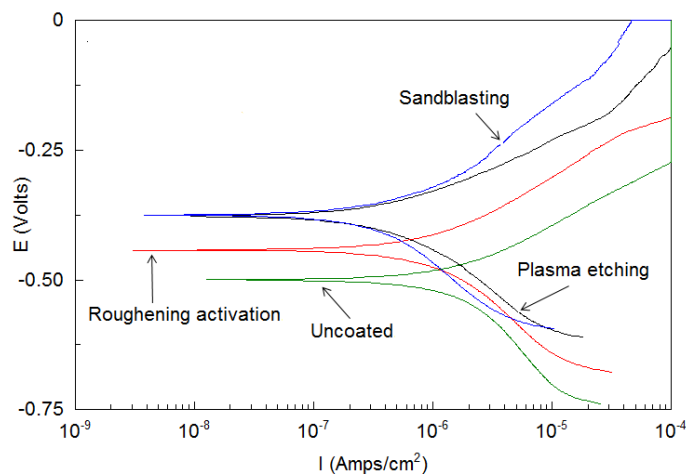


**Figure 5.** The polarization curves for uncoated and coated samples (1, 2 and 3) in 3.5 wt.% NaCl aqueous solution.

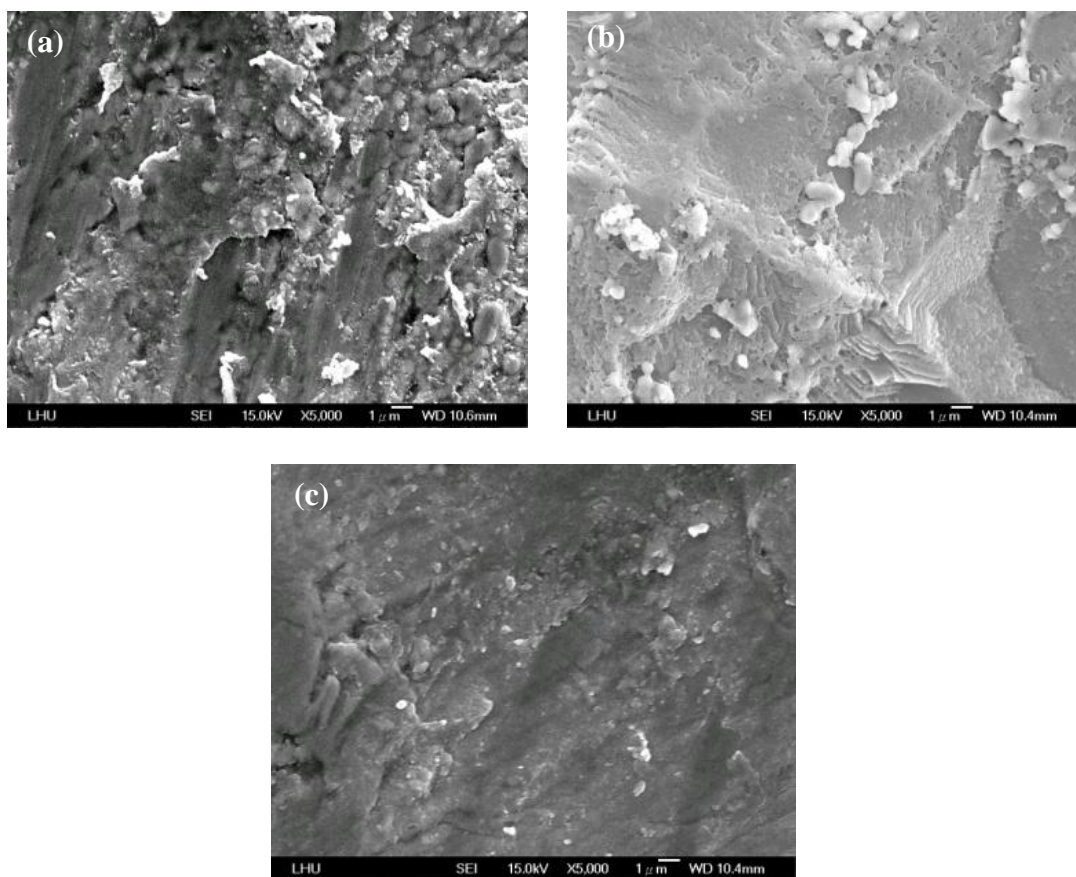


**Figure 6.** SEM micrographs of electroless plated samples after the corrosion test for each substrate pretreatment corresponding to Fig. 5: (a) roughening and then activation (sample 1), (b) sandblasting (sample 2) and (c) plasma etching (sample 3).

**Table 1.** The corresponding polarization resistance ( $R_p$ ), corrosion potential ( $E_{corr}$ ) and the corrosion current density ( $I_{corr}$ ).

|                                     | $\beta_a$<br>(mV) | $\beta_c$<br>(mV) | $\beta$<br>(mV) | $R_p$<br>( $\mu\text{Ohms}/\text{cm}^2$ ) | $I_{corr}$<br>( $\mu\text{Amp}/\text{cm}^2$ ) | $E_{corr}$<br>(Volt) |
|-------------------------------------|-------------------|-------------------|-----------------|---|---|----------------------|
| Uncoated                            | 143.45            | 306.36            | 42.48           | 21.56                                     | 1.97  | -0.5                 |
| Roughening activation<br>(sample 1) | 173.02            | 265.56            | 45.55           | 29.77                                     | 1.53  | -0.44                |
| Sandblasting<br>(sample 2)          | 140.72            | 244.09            | 38.81           | 84.37                                     | 0.46  | -0.37                |
| Plasma etching<br>(sample 3)        | 101.86            | 152.46            | 26.55           | 69.87                                     | 0.38  | -0.37                |

A ball-on-disk tribometer was used to determine the wear behavior of the LCS substrates, without and with a Ni-P film coating. The curves for friction for the coefficient versus the abrasion distance in Fig. 7 show that all coated specimens (samples 1, 2 and 3 are 0.25, 0.23 and 0.16, respectively) have a stable and smaller coefficient of friction than an uncoated LCS substrate (0.36). In particular, the coefficient of friction for the specimen that uses plasma etching (sample 3) has the lowest coefficient of friction of about 0.16. Fig. 8 shows SEM images of the Ni-P film surfaces following the abrasion test, which correspond to Fig. 7. In Fig. 8 (a), sample 1 exhibits severe damage. In Fig. 8 (b), sample 2 has many cracks. In Fig. 8 (c), sample 3 exhibits no significant abrasion or cracking. Therefore, a plasma etching pretreatment produces a Ni-P film that has greater abrasion resistance.

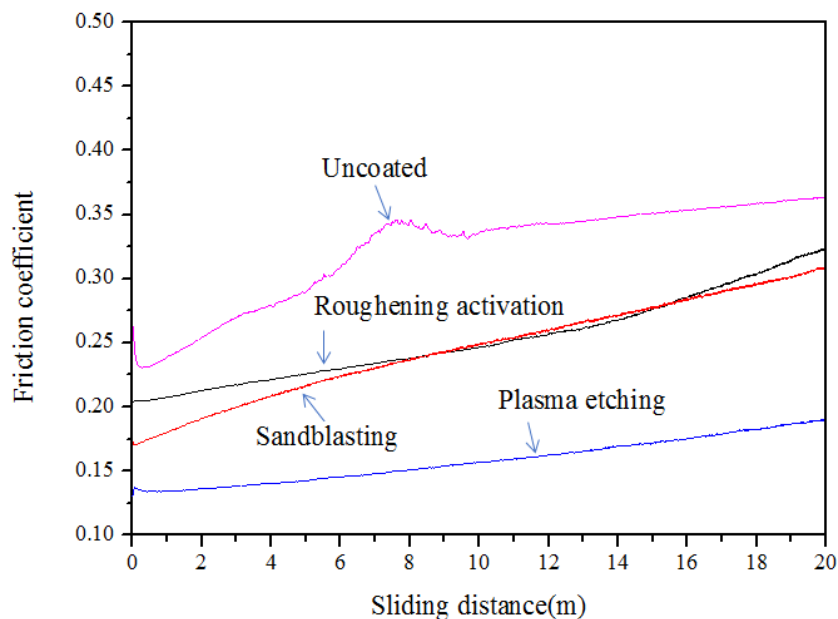


**Figure 7.** A comparison of the coefficients of friction for uncoated and coated samples.



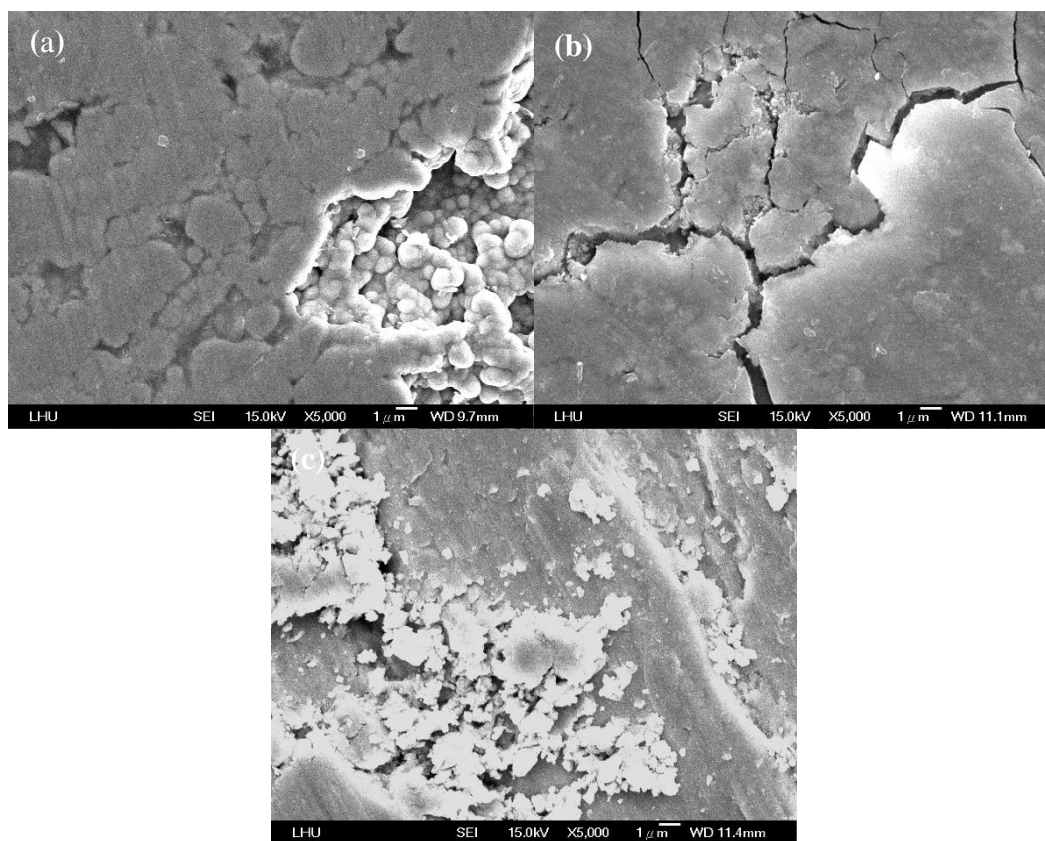


**Figure 8.** SEM micrographs of electroless plated samples after wear testing for each substrate pretreatment: (a) roughening and then activation (sample 1), (b) sandblasting (sample 2) and (c) plasma etching (sample 3), which correspond to Fig. 7.

#### 4. CONCLUSIONS

Before electroless Ni-P plating, the substrate must be roughened and activated. The pretreatment for the low carbon steel (LCS) substrate involves soaking in 15% H<sub>2</sub>SO<sub>4</sub> for 10 min and then in 10% H<sub>2</sub>SO<sub>4</sub> for 30 sec. To reduce chemical pollution, this study replaces the roughening then activation processes with physical sandblasting (emery powder) and plasma etching. The conclusions of this study are as follows:

1. The electroless Ni-P plating using roughening and activation pretreatments for a LCS substrate, gives a film hardness of 254 HV, a coefficient of friction of 0.25 and a corrosion current  $I_{corr}=1.53 \mu\text{A}/\text{cm}^2$ .
2. The electroless Ni-P plating that replace the roughening and activation pretreatments with sandblasting produces a film with a hardness of 293 HV, a coefficient of friction of 0.23 and a corrosion current  $I_{corr}$  of  $0.46 \mu\text{A}/\text{cm}^2$ . The respective improvements are 15.35%, 8% and 69.93%.
3. The electroless Ni-P plating that replaces the roughening and activation pretreatments with plasma etching produces a film a hardness of 299 HV, a coefficient of friction of 0.16 and a corrosion current  $I_{corr}$  of  $0.38 \mu\text{A}/\text{cm}^2$ . The respective improvements are 17.71%, 36%, and 75.16%.

**DISCLOSURE STATEMENT**

No potential conflict of interest was reported by the authors.

**References**

1. A. Farzaneh, M. Sarvari, M. Ehteshamzadeh and O. Mermer, *Int. J. Electrochem. Sci.*, 11 (2016) 9676.
2. W.H. Lee, C.B. Yang, K.T. Chen, H. Chang and C.Y. Hsu, *J. Comput. Theor. Nanosci.*, 13 (2016) 1640.
3. D. Takacs, L. Sziraki, T.I. Torok, J. Solyom, Z. Gacsi and K. Gal-Solymos, *Surf. Coat. Technol.*, 201 (2007) 4526.
4. S.A. Xu and C.S. Liang, *Int. J. Electrochem. Sci.*, 11 (2016) 8817.
5. D. Dong, X.H. Chen, W.T. Xiao, G.B. Yang and P.Y. Zhang, *Appl. Surf. Sci.*, 255 (2009) 7051.
6. M. Zhang, S. Mu, Q. Guan, W. Li and J. Du, *Appl. Surf. Sci.*, 349 (2015) 108.
7. G.W. Kim, Y.S. Kim, H.W. Yang, Y.G. Ko and D.H. Shin, *Surf. Coat. Technol.*, 269 (2015) 314.
8. J. He, D. Sirois, S. Li, M. Sullivan, C. Wikle and B.A. Chin, *J. Mater. Process. Technol.*, 232 (2016) 165.
9. W. Yang, Q. Li, Q. Xiao and J. Liang, *Prog. Org. Coat.*, 89 (2015) 260.
10. K.W. Liew, H.J. Kong, K.O. Low, C.K. Kok and D. Lee, *Mater. Des.*, 62 (2014) 430.
11. P. Sahoo and S. K. Das, *Mater. Des.*, 32 (2011) 1760.
12. T. Xiang, S. Ding, C. Li, S. Zheng, W. Hu, J. Wang and P. Liu, *Mater. Des.*, 114 (2017) 65.
13. Y. Yang, S. Liu, J. Li, X. Bian and Z. Guo, *Surf. Coat. Technol.*, 315 (2017) 484.
14. C.H. Hsu, K.L. Chen, Z.H. Lin, C.Y. Su and C.K. Lin, *Thin Solid Films* 518 (2010) 3825.
15. C.H. Hsu, C.K. Lin, K.H. Huang and K.L. Ou, *Surf. Coat. Technol.*, 231 (2013) 380.
16. H. Zhao and J. Cui, *Surf. Coat. Technol.*, 201 (2007) 4512.
17. L. Li and B. Liu, *Mater. Chem. Phys.*, 128 (2011) 303.
18. C.H. Hsu, K.H. Huang, Y.T. Chen and W.Y. Ho, *Thin Solid Films* 529 (2013) 34.

© 2018 The Authors. Published by ESG ([www.electrochemsci.org](http://www.electrochemsci.org)). This article is an open access article distributed under the terms and conditions of the Creative Commons Attribution license (<http://creativecommons.org/licenses/by/4.0/>).